International Journal of Science and Research (IJSR)
ISSN (Online): 2319-7064
Index Copernicus Value (2016): 79.57 | Impact Factor (2017): 7.296

Combined Spectroscopic and DFT Studies of Pyridoxine

R. Padmavathi[1], S. Gunasekaran[2], B. Rajamannan[3]

[1]Department of Physics, Meenakshi Sundararajan Engineering College, Kodambakkam, Chennai-600024, TN, India

[2]Dean, Research and development St.Peter's institute of Higher Education and Research, St.Peter's University, Avadi, Chennai-600054, TN, India

[3]Engineering physics, FEAT Annamalai University, Annamalai Nagar- 608002, Chidambaram, TN, India

Abstract: ***The Fourier transform Infrared (FTIR) and FT-Raman (FTR) spectra of 4, 5-bis (hydroxymethyl)-2-methylpyridin-3-ol have been recorded in the regions 4000-450 $cm^{-1}$and 4000-500cm^{-1}respectively. Utilizing the observed FTIR and FT-Raman data, a complete vibrational assignment and analysis of the fundamental modes of pyridoxine have been carried out. The optimum molecular geometry, infrared intensities have been calculated by density functional theory (DFT/B3LYP) method with 6-311G (d, p), 6-311++G(d, p) and RHF/6-31G(d, p) basis sets. The complete vibrational assignments were performed on the basis of the potential energy distribution (PED) of the Vibrational modes calculated using Vibrational Energy Distribution Analysis (VEDA 4) program. The calculated HOMO-LUMO energy gap revealed that charge transfer occurs within the molecule. The thermodynamic properties like Entropy, Enthalpy, Specific Heat Capacity and Zero vibrational energy have been calculated. Besides, molecular Electrostatic potential (MEP) was investigated using theoretical calculations. Stability of the molecule arising from hyper conjugative interactions, charge delocalization have been analyzed using NBO (Natural Bond Orbital) analysis***

Keywords: FTIR, FT-Raman, HOMO-LUMO, Mulliken atomic charges, MEP, UV, NBO

1. Introduction

Vitamin B6 is called pyridoxine and it's a white crystalline powder. Its IUPAC name is 4, 5-bis (hydroxymethyl)-2-methylpyridin-3-ol; Pyridoxine chemical formula is $C_8H_{11}NO_3$.Its molecular weight169.18 g/mol. It dissolves in about 4.5 ml water, 90 ml alcohol; soluble in propylene glycol; sparingly soluble in acetone; insoluble in ether, chloroform. Its photosensitive will degrade slowly when exposed to light and preparations should be protected from light and stored in well-closed containers at a temperature less than 40° C, preferably between 15-30° C. Pyridoxine is essential to red blood cell, nervous system, and immune system functions and helps to maintain normal blood glucose levels. B6 is found in bananas, legumes, peanuts, potatoes, wheat cream, brewer's yeast and organ meats (especially liver).Pyridoxine is usually nontoxic. Treating a type of anemia called sideroblastic anemia and seizures in infants. Vitamin B6 plays a vital role in several enzymatic reactions. It acts as a coenzyme for numerous enzyme-catalyzed reactions such as transamination, α- and β-decarboxylation's, β- and γ-eliminations, and racemization's and aldol reactions [1]. Cinta et al. [2] investigated the pH dependence of the Raman and SERS spectra of pyridoxine hydrochloride and assigned the vibrational modes by the aid of ab initio (3-STO) and semi empiric (PM3) calculations. Srivastava et al. [3] calculated the harmonic vibrational wavenumbers for the optimized geometry pyridoxine, using density functional theory method B3LYP/ 6-311++G** level of theory. But the geometry optimization was not performed by torsion potential energy surfaces scan studies through the dihedral angles. It is well known that vibrational wavenumbers are strongly dependent on the conformational changes, for this reason, vibrational behavior of the lowest energy conformer of pyridoxine monomer was investigated. B.Atak-Bulbul et al.[4] investigate the possible stable conformers of free pyridoxine molecule and searched by means of torsion potential energy surfaces scan studies through the dihedral angles, D1 (9H-8O-4C-3C), D2 (12H-10C-5C-6N), D3 (15O-14C-2C-1C) and D4 (O22-19H-3C-2C). The final Geometrical parameters for the obtained stable conformers were determined by means of geometry optimization, carried out at DFT/B3LYP/6-311G++ (d, p) theory level. [5] G. A. Gamov et al. investigate on geometric optimization for the neutral, zwitterionic, and protonated forms of pyridoxine in vacuum and in water with a solvent within the polarizable continuum model (PCM). The structural parameters are optimized for pyridoxine complexes in the neutral and zwitterionic forms with 4-10 water molecules. An analysis was also performed to find the number of molecules of the solvent set by the model affects the agreement between the calculated and experimental NMR spectra. QuassilaAttoui-Yahia [6] investigate the occurrence of hydrogen bonding (HB) interactions, including intra and intermolecular HB, in the stability of the inclusion complex Pyridoxine/β-cyclodextrin, conformational research achieved with PM3MM, ONIOM-2 and DFT (B3LYP/6-31Gd) calculations gave a geometrical structure for the lowest energy complex in which the pyridine ring of the guest is self-imbedded inside the hydrophobic cavity of β-CD [7]. Electronic and spectroscopic properties of vitamin B6 (pyridoxine) and some of its main charged and protonated/deprotonated species are explored using hybrid density functional theory (DFT) methods including polarized solvation models found that the dominant species at low pH is

the N1-protonated form and, at high pH, the O3′-deprotonated compound. Literature survey reveals that to the best of our knowledge no DFT/B3LYP with 6-311++G (d.p), 6-311G (d, p) and RHF/6-31G(d, p) basis sets calculations of pyridoxine have been reported so far. Therefore an attempt has been made in the present study the detailed theoretical DFT and Experimental (FTIR, FT-Raman, UV) spectral investigation of pyridoxine. The FT-IR and FT Raman spectra of this compound have been stimulated with the use of the standard 6-311++G (d.p), 6-311G (d, p) and RHF/6-31G(d, p) basis sets.The results of the theoretical and spectroscopic studies are reported here in. Detailed interpretations of the vibrational spectra of pyridoxine have been made on the basis of the calculated potential energy distribution (PED).By using DFT (B3LYP) method, we have calculated the geometric parameters in the ground state, thermodynamic properties, vibrational energies, rotational constant, entropy, molar capacity and thermal energies by using Gaussian 03 programs. In addition, the energies of the highest occupied molecular orbital (HOMO) and the lowest unoccupied molecular orbital (LUMO) of pyridoxine in the ground state are calculated by using B3LYP method with 6-311++G (d, p) basis set. UV-visible spectrum, Mulliken atomic charges and Natural Bond Orbital (NBO) analysis were also calculated.

2. Experimental Details

The Spectroscopic pure samples of pyridoxine was procured from a pharmaceutical company with more than 99% purity and used as such for the spectral recordings. FTIR ATR spectrum was recorded using Perkin-Elmer spectrum two FTIR spectrometer with ATR accessory, in the range of 4000-450 cm^{-1} and UV – visible spectral analysis was made using Perkin Elmer –Lambda 35 UV WINLAB V 6.0 spectrometer in the region 200-800 nm. These spectral recordings were carried out at Sophisticated Analytical Instrumentation Facility (SAIF), St .Peter's University, Avadi, and Chennai, India. FT-Raman spectrum was recorded using 1064 nm line Nd: YAG laser operating at 200mw on Bruker RFS 27 spectrometer with 8 scans at a resolution of $2cm^{-1}$ in the range of 4000-50 cm^{-1} at Sophisticated Analytical Instrumentation Facility (SAIF), IIT Madras, India.

3. Computation details

The quantum chemical theoretical calculations were performed by using DFT-B3LYP levels on MSRC3 Intel ® core (TM) i5-3470 CPU @ 3.20GHz personal computer. The primary task for the computational work was to determine the optimized geometry of the compound using Gaussian 03 software [8] programs, invoking gradient geometry optimization [9]. DFT calculations were performed using Becker's three-parameter [10, 11] hybrid model using Lee-yang-Parr (B3LYP) [12] correlation functional method. The computations were performed at RHF/6-31G (d, p), B3LYP/6-311++G(d, p), B3LYP/6-311G(d, p) basis sets [13, 14] have been utilized for the computation of molecular structure optimization, geometrical parameters , vibrational scaled wave numbers of the normal modes, IR intensities, atomic charges and thermodynamic parameters of the title compound. The complete assignments were performed on the basis of the potential Energy distribution Analysis (VEDA) 4 program.

4. Results and Discussion

4.1 Molecular geometry

The molecular structure of Pyridoxine belongs to C_1 point group symmetry. All vibrations are active in both IR and Raman. The optimized molecular structure of pyridoxine is shown in the Fig 1.The optimized geometrical parameters such as bond lengths and bond angles obtained by the DFT/B3LYP methods with the 6-311G (d, p), 6-311++G(d, p) and RHF/ 6-31G(d, p) respectively are shown in table 1. The various bond lengths and bond angles are found to be almost same at B3LYP/ 6-311G (d, p), 6-311++G(d, p) methods. The bond length between atoms C2-C11 was calculated as in the range of 1.337° and 1.42°by using the DFT/B3LYP with two different basis sets and 1.3944° by RHF method. Both methods are in good agreement with experimental data 1.394°. The distance between C4-C5 was calculated as in the range of 1.3371° and 1.42° by using DFT/B3LYP with two different basis sets and corresponding RHF value is 1.3834° and both the methods are in good agreement with experimental values 1.394°. The bond angle between C3-C4-C5 in RHF and B3LYP methods are 120.0004°, 123.5°, and 123.0049° which match exactly with the experimental value of 123.3°. The bond angle between C5-C4-C16 in RHF is 120.8365° and in B3LYP methods are 119.9941°, 118.2489° which match exactly with the experimental value 120.3°. The dihedral angle between C6-C5-C8-C11 by B3LYP/6-311G (d, p) is 180 and B3LYP/6-311++G(d, p) value 179.447 and RHF/6-31G(d, p) value is 179.5449 respectively. The calculated geometric parameters can be used to determine the other parameters of PYR. The optimized bond lengths are larger than the experimental values as the theoretical calculations result from isolated molecules in gaseous state, Bond angles and dihedral angles were referred from [15].

Figure 1: Molecular Structure of 4, 5-bis (hydroxymethyl)-2-methylpyridin-3-ol

4.2 Vibrational spectral analysis

The FTIR-ATR spectrum of a compound is the superposition of the absorption bands of specific functional groups. By observing the position, shape and relative intensities of the vibrational bands in FTIR spectra of the powder molecules of Pyridoxine vibrational band assignment has been made and summarized in Table-1. The FTIR-ATR and FT-Raman spectra of Pyridoxine by experimental and theoretical spectrum are shown in Fig.2-7.and the description of various band assignments are as follows.

4.2.1 O-H Vibrations

The O-H group vibrations are likely be the most sensitive to the environment, so they show pronounced shifts in the spectra of the hydrogen bonded species. The O-H stretching vibrations are usually observed in the region 3500cm^{-1}[16]. In the present work O-H stretching vibrations are occur at 3322, 3232cm^{-1} in FTIR and 3233 occur in FT- Raman spectrum. Theoretically the scaled B3LYP/6-311++G (d, p) values are occur at 3340, 3335, 3323cm^{-1}and corresponding B3LYP/6-311G(d, p) Values are 3343, 3330, 3329cm^{-1} respectively. Kanagathara et al. [17] have also observed O-H stretching at 3882cm^{-1} in FTIR spectrum. Santhana Krishnan et.al [18] too have observed O-H vibration at 3660cm^{-1}in FTIR.

4.2.2 C-H Vibrations

The hetero aromatic structure shows the presence of C-H stretching vibrations in the region 3100-3000 cm^{-1} which is the characteristic region for the ready identification of C-H stretching vibration [19]. The C-H stretching is typically exhibited as a multiplicity of weak to moderate bands, compared with the aliphatic C-H stretching. In our present investigation 3086, 2815, 1827, 1731cm^{-1}occur at FTIR and 3099, 2975, 2934, 2901, 2865, 2828cm^{-1} occur at FT-Raman are assigned to C-H stretching vibrations. The B3LYP/6-311++G (d, p) value are 2767, 2726, 2690, 2687, 2648, 2622, 2610, 2590 cm^{-1}are assigned to C-H stretching and B3LYP/6-311G(d, p) value are 2735, 2728, 2683, 2657, 2647, 2637, 2610,
2609 cm^{-1} respectively. As indicated by PED these modes involve maximum contribution of about 96% suggesting that they are due to pure stretching modes. Arivazhagan et.al [20] have also observed C-H stretching at 3000, 2983cm^{-1} in FT-Raman spectra. Ramkumar et, al, [21] have reported C-H stretching at 3167, 2933cm^{-1} in FTIR and at 2941 cm^{-1} in FT-Raman spectra respectively.

4.2.3 C-C Vibrations

The C-C aromatic stretching vibrations give rise to characteristic bands in the spectral range from 1600-1400 cm^{-1}[22].C-C Stretching vibrations for title compound is observed at 1542cm^{-1}FTIR and at 1499, 1232cm^{-1} in FT- Raman spectra. Theoretically C-C stretching vibration are observed at 1429, 1223, 1135, 1067 cm^{-1} in B3LYP/6-311++G (d.p) and B3LYP/6-311G (d, p) values are 1433, 1246, 1117, 1081 cm^{-1} respectively.

4.2.4 N-C Vibrations

N-C stretching vibrations are occur in the region of 1000-1350 cm^{-1}. In the present work N-C stretching vibrations are occurred at 1542, 1462 in FTIR and 1449, 1392 are observed at FT-Raman respectively. Theoretically N-C stretching vibrations occur at 1429, 1323, 1135, 1112, 1067 in B3LYP/6-311++G (d, p) and 1433, 1332, 1117, 1114, 1081 in B3LYP/6-311G(d, p) respectively.

4.2.5 C-O vibration

The C-O stretching vibration is normally at 1320–1210 cm^{-1} due to C-O stretching vibrations [23]. Accordingly in the present study the C-O stretching vibration of PYR are observed at 1214 cm^{-1} in FTIR spectrum, and medium band observed at 1232, 1217 cm^{-1} in Raman spectrum. The theoretically computed frequencies at 1223, 1218, 1607 cm^{-1} and at B3LYP/6-311G (d, p) and 1246, 1220 cm^{-1} in 6-311++G(d, p) basis sets respectively

4.3 Thermodynamic Properties

The statistical thermo chemical analysis of pyridoxine was performed considering the molecule to be at room temperature 298.15 K and one atmospheric pressure. All the thermodynamic data supply helpful information for further study of the title molecule. Using B3LYP/6-311++G (d, p) and RHF/6-31G(d, p) several thermodynamic properties such as heat capacity at constant pressure (Cp), entropy (S) and enthalpy (ΔH) for the title compound were evaluate from the theoretical harmonic frequencies obtained from the temperature 100-1000K and are listed in Table 3.

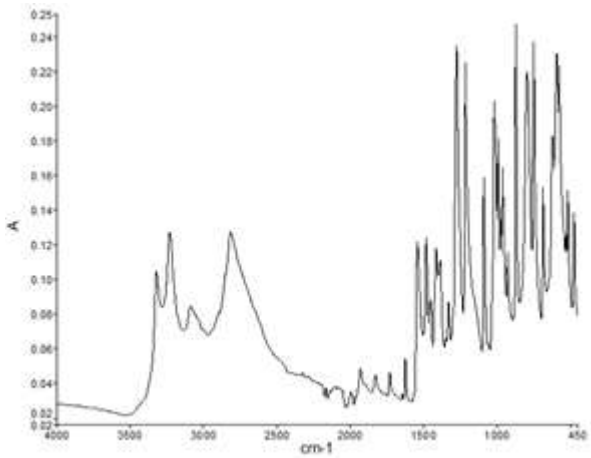

Figure 2: FTIR experimental Spectrum of pyridoxine

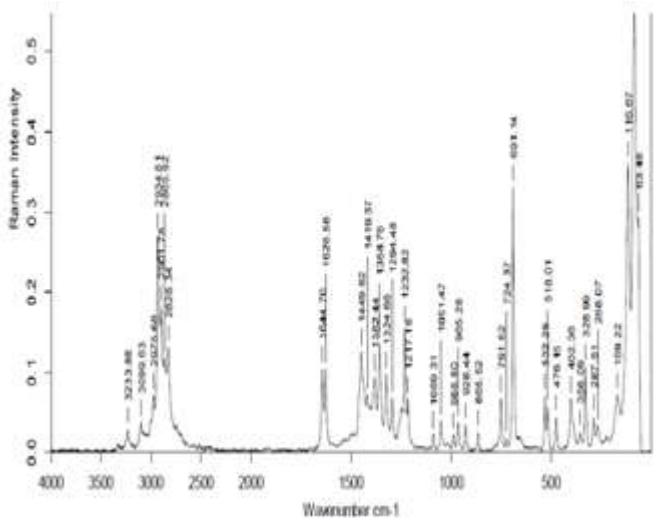

Figure 3: FT-Raman experimental Spectrum of pyridoxine

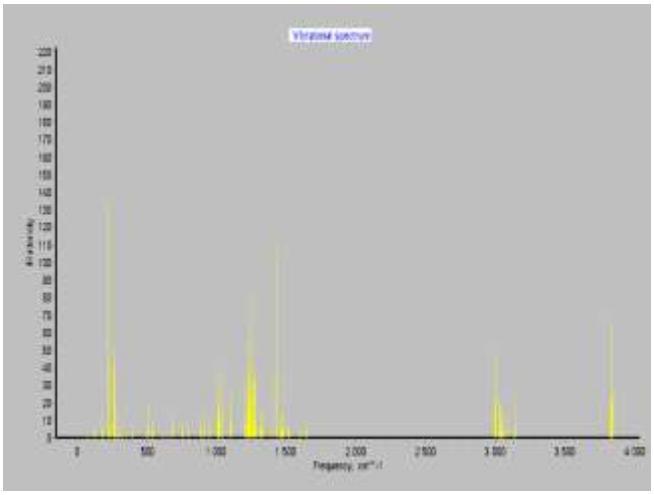

Figure 4: FTIR theoretical Spectrum of pyridoxine by B3LYP/6-311++G (d, p)

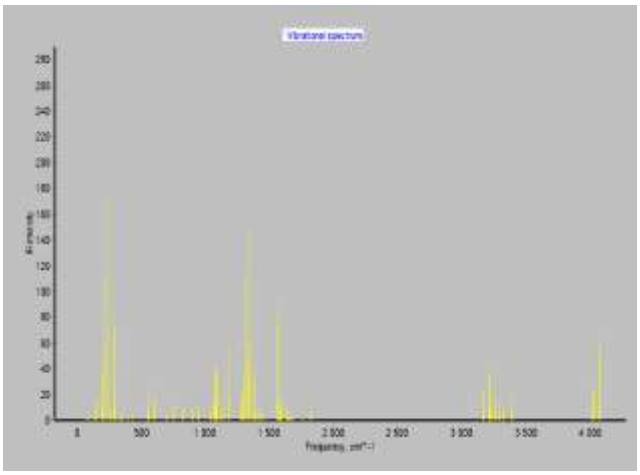

Figure 5: FTIR theoretical Spectrum of pyridoxine by B3LYP/6-311G (d, p)

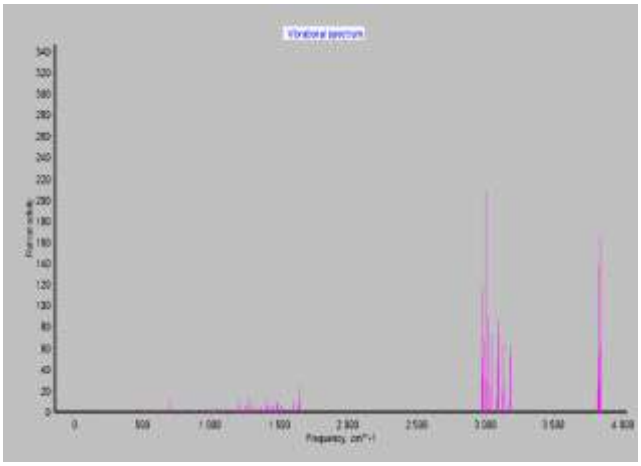

Figure 6: FT-Raman theoretical Spectrum of pyridoxine by B3LYP/6-311++G (d, p)

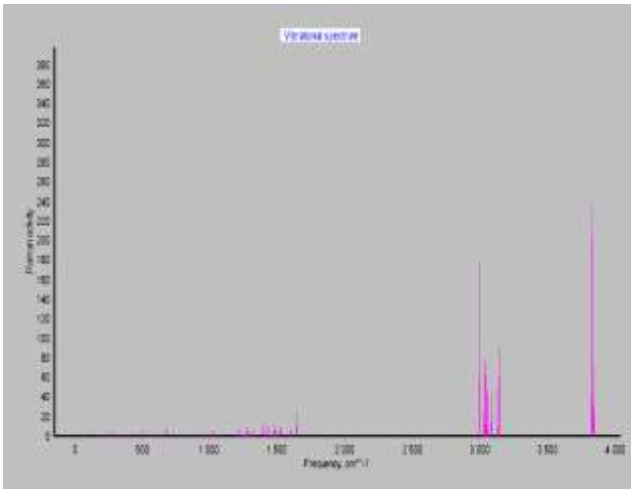

Figure 7: FT-Raman theoretical Spectrum of pyridoxine by B3LYP/6-311 G (d, p)

From this table it is evident that the properties increase with increase in temperature due to the fact that the vibrational intensities of the molecules increase with temperature. The correlation between these thermodynamic properties and temperature are fitted by quadratic formula as follows and corresponding fitting factors (R^2) for these thermodynamic properties were found to be 0.99978, 0.99986 and 0.99962.The temperature dependent correlation graphs are shown in Fig 8.The ZPVE'S energy is much lower in the DFT/B3LYP level at 6-311++G (d, p) basis set than the other basis sets [24].The bigger value of ZPVE's of Pyridoxine is 125.83731(Kcal/Mol) obtained by RHF/6-31G(d, p) method. The minimum value of entropy are calculated in 107.581 at RHF/6-31G (d, p) and maximum one was calculated at 109.551 at B3LYP/6-311++G(d, p) in pyridoxine molecule. The transitional and rotational thermal energies, molar capacity are also same for B3LYP level with all basis sets are shown in table 5.The Homo-Lumo energies, energy gap, chemical hardness, electronegativity, electrophilicity, chemical potential are also calculated and shown in table 4.

$S=231.64782+0.82041T-2.18228*10E-4*T^2$ ($R^2=0.99978$)

$C_P=29.23246+0.66311T-2.72477*10E-4*T^2$ ($R^2=0.99986$)

ΔH=-8.47221+0.09915T+1.181577*10E-4* T^2
(R^2 =0.99962)

4.4 Mulliken population analysis

The Mulliken charge is directly related to the vibrational properties of the molecule and quantifies how the electronic structure charges under atomic displacement. It is therefore related directly to the chemical bonds present in the molecule. It affects dipole momentum polarizability electronic structure and more properties of molecular system [25]. The Mulliken analysis was performed on the title molecule by B3LYP and RHF methods using 6-311++G (d, p), 6-311G(d, p) and6-31G (d, p) as the basis set and presented in the table [6]. The illustration of Mulliken atomic charge plotted is shown in Fig.9. The oxygen atoms O7, O10, O12 have charges _0.270178, _0.25063 and _0.236904 respectively in the B3LYP method, of which O7 has the highest negative value. N3 as the least negative value of _0.001575 by B3LYP method and all the hydrogen atoms have positive values and the H23 has the highest positive values. The net charge of hydrogen atoms is 2.187436in B3LYP method. The presence of negative charge on nitrogen and oxygen atoms and the net +ve charge on hydrogen atoms may suggest the formation of intramolecular interaction in solid forms. The advantage of population analysis is that it is useful for comparing changes in partial change assignment between two different geometries with the same size basis sets.

4.5 UV-Visible Spectral analysis

UV-Visible spectral analysis of PYR has been done experimentally and theoretically .Time –dependent density functional theory (TD-DFT) is a powerful tool for investing the static and dynamic properties of the molecules in their excited states [26].UV spectral studies are very useful in determining the transmittance and absorption on an optically active material [27].Fig.10 Shows the UV spectrum of pyridoxine and Table 7 shows the experimental and calculated absorption wavelength (λ), excitation state, Oscillator strength (f), electronic absorption value and transition of pyridoxine. According to Franck-Condon principle, the maximum absorption peak (λ_{max}) corresponds to vertical excitation. Theoretical calculations predicts one intense electronic transition at 204nm with an oscillator strength f=0.2853 and electronic absorption value 6.0675Ev. which is in good agreement with the experimental value 477 nm corresponding to HOMO–LUMO+1, HOMO-LUMO+2, HOMO-LUMO+3, HOMO -LUMO+4 transition. Another peak at 201 nm with oscillator strength 0.0030 and electronic absorption value 6.1390eV corresponds to the second excited state with transitions HOMO-LUMO+1 to HUMO-LUMO+6, which is in good agreement with the experimental value 268 nm. The third peak 184nm at 6.7124eV with oscillator strength 0.0204 corresponds the third excited state and the corresponding transition occurs between HOMO-LUMO +1 TO HOMO-LUMO+8.

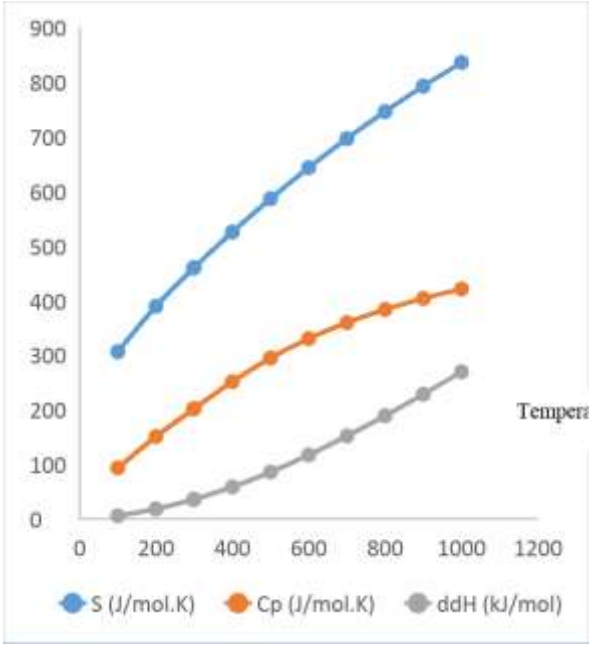

Figure 8: Correlation graph between entropy, heat capacity and enthalpy with temperature

4.6 HOMO-LUMO analysis

The HOMO energy is directly related to the ionization potential while, LUMO energy to electron affinity .HOMO energy and LUMO energy are theoretically calculated to be -.0.24021 a.u and -0.04197 a.u respectively. The energy gap is 0.19824 a.u in B3LYP method. Fig 6 represents the pictorial illustration of the frontier molecular orbital's and their respective positive and negative regions. Several ways calculate the HOMO- LUMO energies. The simplest one involves the difference between highest occupied molecular orbital HOMO the lowest unoccupied molecular orbital LUMO of neutral system. This is a key parameter in determining molecular properties. Highest occupied molecular orbital and lowest unoccupied molecular orbital are very important parameters for quantum chemistry. We can determine the way molecule can interact with other species; hence they called the frontier orbital. Frontier molecular orbitals play an important role in the electric and optical properties [28] as well as in UV-Vis spectral and chemical reactions. The energy of HOMO is directly related to the ionization potential, LUMO energy is directly related to the electron affinity.

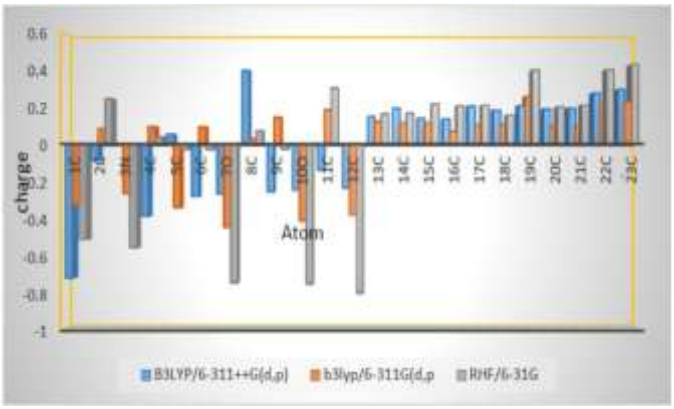

Figure 9: Plot of Mulliken charges and Atoms by B3LYP/ 6-311++G(d, p) , 6-311G(d, p). RHF/6-31 G (d, p)

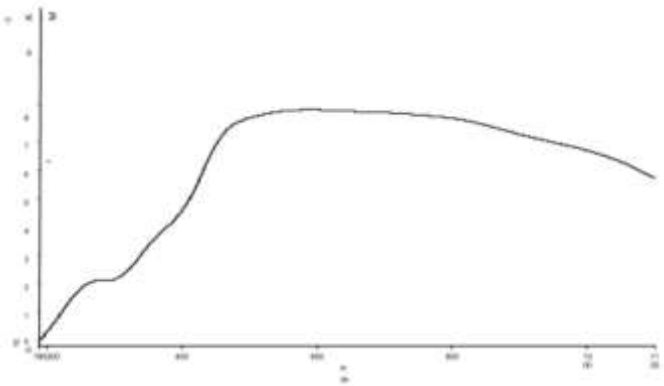

Figure 10: UV-Visible spectrum of Pyridoxine

Energy difference between HOMO and LUMO orbital is called as energy gap that is an important stability for structure [29] and reveals the chemical activity of the molecule .The HOMO –LUMO orbitals computed at B3LYP level with 6-311G(d, p) is shown in fig 8. The lower HOMO-LUMO energy gap explains the eventual charge transfer interactions taking place within the molecule. It is an established fact that a large frontier orbital energy gap implies high kinetic stability and low chemical reactivity. Because it is energetically unfavorable to add electrons to a high-lying LUMO to extract electrons from low–lying HOMO [30] for PYR. The HOMO-LUMO energy gap reflects the chemical activity of the molecule. The LUMO as an electron acceptor represent the ability to obtain an electron. The HOMO represents the ability to donate an electron.

4.7 Molecular Electrostatic Potential

Molecular electrostatic potential (MESP) at a point in the space around a molecule gives an indication of the net electrostatic effect produced at that point by the total charge distribution (electron+ nuclei) of the molecule and correlates with the dipole moments, electronegativity, partial charges chemical reactivity of the molecules. It provides a visual method to understand the relative polarity of the molecule. Thus, MESP serves as a useful quantity to explain hydrogen bonding, reactivity and structure–activity relationship of molecule including biomolecules and drugs [31-33].The different values of the electrostatic potential, at the surface are represented by different colour's; red represents regions of most negative electrostatic

Excited state = -0.04197 a. u

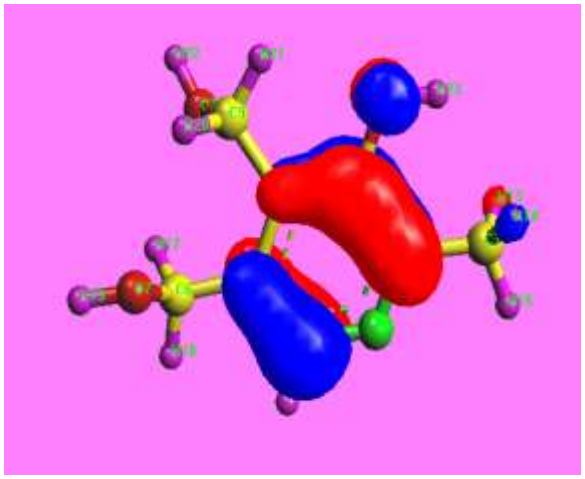

Energy gap = 0.19824 a.u

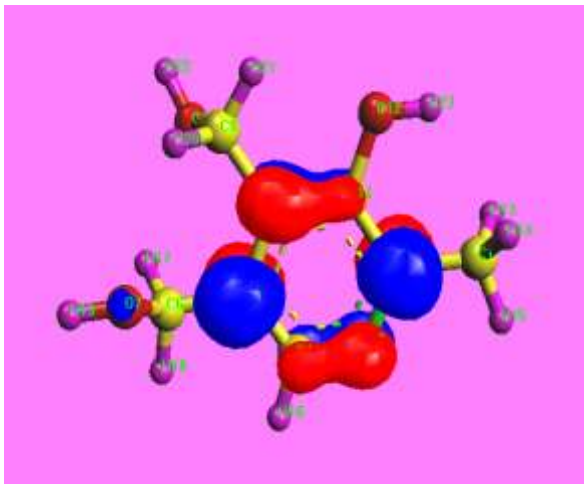

Ground state -0.24021a.u

Figure 11: The atomic orbital composition of the frontier molecular orbital for pyridoxine potential, which corresponds to an attraction of the proton by the concentrated electron density in the molecule; blue represents regions most positive electrostatic potential and green represents regions atoms of zero potential. Potential increases in the order red<orange<yellow<green<blue. The atoms O12, O10, O7 were electrophilic sites. Nitrogen atom N3 was a nucleophilic site from these results; one can say that the nitrogen atom and hydrogen atoms indicate strongest attraction, while oxygen atoms indicate strongest repulsion. These sites give information about the region from where the compound can have intermolecular interactions.

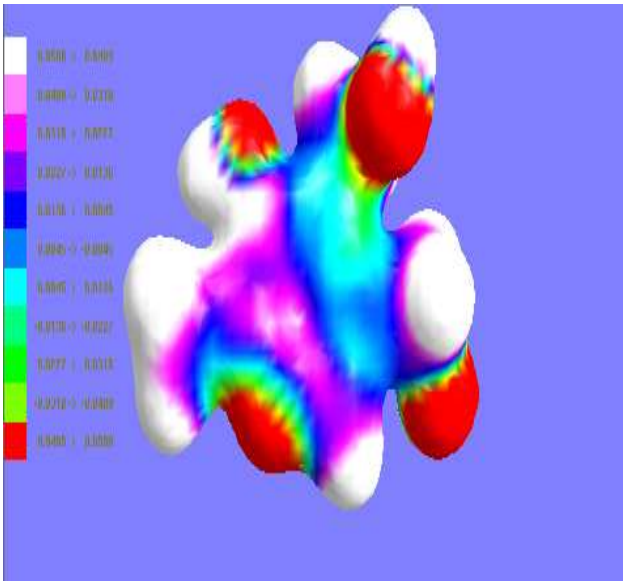

Figure 12: Electrostatic potential surfaces of PYR by B3LYP/6-311++G (d, p)

The site corresponding to the benzene ring is highly active and it can play an important role in the activity of PYR. The figures confirm the different positive and negative sites of the molecule in accordance with the total electron density surface. Such electrostatic potential surfaces have been for PYR in B3LYP/6-311++G (d, p) shown in fig [11].

4.8 NBO analysis

NBO analysis provides the most accurate possible 'natural Lewis structure' picture of φ, because all orbital details are mathematically chosen to include the highest possible percentage of the electron density. A useful aspect of NBO method is that it gives information's about interactions in both filled and virtual orbital spaces that could enhance the analysis of intra and inter molecular interactions. The second Fock matrix was carried out to evaluate donor-acceptor interactions in the NBO analysis. The interactions result is a loss of occupancy from the localized NBO of the idealized Lewis structure into an empty non-Lewis orbital. For each donor (i) and acceptor (j), the stabilization energy E^2 associated with the delocalization i $\rightarrow$ j is estimated as

$$E^{(2)} = \Delta E_{ij} = q_i \frac{F(i,j)^2}{(\varepsilon_j - \varepsilon_i)}$$

Where q_i is the donor orbital frequency, εi and ε_j are diagonal elements and F (i, j) is the off diagonal NBO Fock matrix element. NBO analyses provide an efficient method for studying intra and inter molecular bonding and interaction among bonds and also provide a convenient basis for investigating charge transfer or conjucative interaction molecular systems. Some electron donor orbital, acceptor orbital and the interacting stabilization energy resulted from the second order micro-disturbance theory are reported. The larger E(2) value, the more intensive is the interaction between the electron donor an acceptors, i.e the more donating tendency from the form the electron donors to electron acceptors and the greater extent of conjucation of the whole system. Delocalization of electron density between occupied Lewis type (bond or lone pair) NBO orbitals and formally unoccupied (anti-bond or Rydberg) non Lewis NBO orbitals correspond to a stabilizing donor-acceptor interaction. NBO analysis has been performed on the molecule at the B3LYP/6-311++G (d, p) level in order to elucidate the intra molecular, rehybridization and delocalization of electron density with in the molecule. The interaction between lone pair LP (3) of type O12 of type O11 with σ* (C2-C11) results in a stabilization energy of 28.67KJ/mol and lone pair LP (2) of type O10 with σ* (C6-O7) results in stabilization energy of 10.02KJ/mol. These indicate larger delocalization. The intramolecular hyperconjugative interaction of σ (C4-C5) to σ* (C6-O7) leading to strong stabilization of 10.81KJ/mol. The intramolecular hyperconjugative interaction of σ (C5-C6) to σ*(C5-C8) and σ (C5-C8) to σ*(C8-C11) leads to stabilization of 8.08 and 8.06KJ/mol respectively. These interactions are observed as increase in electron density in antibonding orbital that weakens the respective bonds. These charge transfer interactions in pyridoxine are responsible for biological properties. Hence pyridoxine structure is stabilized by these orbitals Interactions. In pyridoxine, the oxygen has larger polarization co-efficient because it has the higher electronegativity. The calculated values of E (2) are given in Table [8].

5. Conclusion

A complete vibrational analysis of 4, 5-bis (hydroxymethyl)-2-methylpyridin-3-ol is performed by DFT/B3LYP level with 6-311++G (d.p), 6-311G(d, p) and RHF/6-31G(d, p) basis sets. On the basis of calculated potential energy distribution results assignments of the fundamental vibrational frequencies have been made unambiguously. The calculated geometrical parameters were found to be in good agreement with the experimental data. Thermodynamic properties zero point Vibrational energies rotational constant, thermal energy, molar capacity are discussed elaborately. The stability and intermolecular interactions have been interpreted by NBO analysis and the transitions give stabilization to the structure have been identified by second perturbation energy calculations. The lowering of HOMO-LUMO energy gap, a quantum chemical descriptor, explains the charge transfer interactions taking place within the molecule. The Mulliken atomic charges gives the proper understanding of the atomic theory and the energies of important MOs and the λmax of the compounds were also evaluated from TD-DFT method.

6. Acknowledgement

The authors are thankful to St. Peter's Institute of Higher Education and Research for recording FTIR-ATR and UV-Visible spectrum. The author is thankful to Management Meenakshi Sundararajan Engineering College (MSEC) for showing a keen interest in this work.

References

[1] G.S. Kiruba and M.W. Wong, J. Org. Chem., 68, 2874 (2003).
[2] S. Cinta, C. Morari, E. Vogel, D. Maniu, M. Aluas, T. Iliescu, O. Cozar and W. Kiefer, Vib. Spectroscope, 19, 329 (1999).
[3] M. Srivastava, P. Rani, N.P. Singh and R.A. Yadav, Spectrochim. Acta A, 120, 274 (2014).
[4] B. ATAK-BULBUL* and S. AKYUZ, *Asian Journal of Chemistry; Vol. 26, Supplementary Issue (2014), S299-S304*
[5] G. A. Gamov, V. V. Aleksandriiskii and V. A. Sharnin Journal of Structural Chemistry. Vol. 58, No. 2, pp. 276-282, 2017.
[6] Ouassila Attoui-Yaia, Djameleddinekhatmi-Khairedine Kraim, Fouad Ferkous Volume 47, February 2015, Pages 91-98.
[7] Mikael Ristila, Jon M. Matxain, Åke Strid, and Leif A.Eriksson J, Phys.Chem B 2006, 110, 16774-16780
[8] M. J. Frisch, G. W. Trucks, H. B. Schlegel, G. E. Scuseria, M.A.Robb, J. R. Cheeseman, G. Scalmani, V. Barone, B. Mennucci, G. A. Petersson H. Nakatsuji, M. Caricato, X. Li, H. P. Hratchian, A. F. zmaylov, J. Bloino, G. Zheng, J. L. Sonnenberg, M. Hada, M. Ehara, K. Toyota, R. Fukuda, J. Hasegawa, M. Ishida, T. Nakajima, Y.Honda, O. Kitao, H. Nakai, T.Vreven, J. A. Montgomery, Jr., J. E. Peralta, F. Ogliaro, M. Bearpark, J. J. Heyd, E. Brothers, K. N. Kudin, V. N.Staroverov, T. Keith, R. Kobayashi, J. Normand, K. Raghavachari, A. Rendell, J. C. Burant, S. S. Iyengar, J. Tomasi, M. Cossi, N. Rega, J. M. Millam, M. Klene, J. E. Knox, J. B. Cross, V. Bakken, C. Adamo, J. Jaramillo, R. Gomperts, R. E. Stratmann, O. Yazyev, A. J. Austin, R. Cammi, C. Pomelli, J. W. Ochterski, R. L. Martin, K. Morokuma, V. G. Zakrzewski, G. Voth, P. Salvador, J. J. Dannenberg, S. apprich, A.D. Daniels, O. Farkas, J. B. Foresman, J. V. Ortiz, J. ioslowski, and D. J. Fox, Gaussian Inc., Wallingford CT, 2013.
[9] H.B.Schlegel, J.Comput.chem.3 (1982) 214-218.
[10] A.D.Becke, Phys, Rev.A 38 (1988) 3098-3100
[11] C.Lee, W.Yang, R.G.Parr, Phys.Rev.B 37 (1988) 785-789.
[12] B.G.Johnson, M.J.Frisch, chem. Phys.Lett.216 (1993) 133-140.
[13] W.J. Hehre, L.Random, P.V.R. Schleyer, A.J. Pople, Ab Initio Molecular Orbital Theroy, Wiley, New York, 1989.
[14] Z. Dega-Szafran, A. Katrusiak, M. Szafran, j.Mol, Struct, 741 (2005) 1-9.
[15] Mayuri Srivastava, P. Rani, N. P. Singh, R. A. Yadav, Science Direct, Vol.120:274-286, 2014.
[16] D. Sajan, I. Hubert Joe, V. S. Jayakumar, J. Zabski, J.Mol.struc.785 (2006)43-53
[17] N. Kanagathara, M. K. Matchewka, M. Drozd, N. G. Renganathan, S. Gunasekaran, G. Anbalagan, Spectrochim.Acta A 112 (2013) 343-350
[18] V. Santhana Krishnan, S. Sampath Krishnan, S. Muthu, S.Renuga, Spectrochim. Acta A 115 (2013) 191-2011
[19] G.Varanyi, Assignments for Vibrational Spectra of Seven Hundered Benzene Derivatives, Vol.1-2, Academic Kiaclo, Budapet, 1973.
[20] M.Arivazhagan , D.AnithaRexalin, Spectrochim, Acta A 83 (2011) 553-560.
[21] G.R .Ramkumaar, S.Srinivasan, T.J.Bhoopathy, S.Gunasekaran, Spectrochim, Acta A 99 (2012) 189-195
[22] Erdogdu, O. Unsalan, M. Amalanathan, I. Hubert Joe, J. Mol. Struct. 980 (2010) 24–30.
[23] D. Mahadevan, S. Periandy, S. Ramalingam, Spectrochim. Acta Part A 79 (2011) 962–969.
[24] M.Govindarajan, M.Karaback, Spectrochim, Acta Part A 96 (2012) 421-435.
[25] A .Dreuw, M.Head-Gordon, Chem, Rev. 105 (2005) 4009- 4037.
[26] D.Jacquemin. J.Preat, E.A. Perpete, Chem Phys Lett. 40(2005) 254-259.
[27] D.F.V.Lewis , C.Ioannide , D.V.Parke, Venobiotica 24 (1994)401-408.
[28] J .Aihara, J.Phys.Chem.A 103 (1999) 7487-7495.
[29] M.Arivazagan , J.J eyavijiayan, Spectrochim. Acta Part A 79 (2011)376-383
[30] Chidangil S, Shukla M K & Mishra P C, J Mol Model, 4 (1998) 250
[31] Pepe G, Siri D & Reboul J P, J Mol Struc (Theochem), 256 (1992) 175
[32] Anbha Srivastava, Poonam Tandon, Ayala AP & Sudha Jian, Vib Spec, 56 (2011) 82

Table 1: Geometrical parameter optimized in Pyridoxine by B3LYP with B3LYP/6-311 G(d, p), B3LYP/6-311G(d, p), RHF/6-31G(d, p)

Parameters	B3LYP/6-311G(d, p)	B3LYP/6-311++G(d, p)	RHF/6-31G(d, p)	Expt
C1-C2	1.497	1.475	1.5027	
C1-C13	1.1129	1.113	1.0871	
C1-C14	1.113	1.113	1.0866	
C1-C15	1.113	1.113	1.0787	
C2-C3	1.26	1.358	1.3266	1.34
C2-C11	1.337	1.42	1.3944	1.394
C3-C4	1.26	1.358	1.3307	1.34
C4-C5	1.3371	1.42	1.3834	1.394
C4-C16	1.1	1.1	1.071	
C5-C6	1.497	1.497	1.501	
C5-O8	1.337	1.1901	1.3971	
C6-C7	1.402	1.421	1.4428	
C6-C17	1.113	1.111	1.0795	
C6-C18	1.113	1.111	1.0827	
C7-H19	0.942	0.942	0.9515	
O8-O9	1.497	1.497	1.5036	
O8-C11	1.0287	1.42	1.385	
O9-N10	1.402	1.421	1.4452	
O9-H20	1.1129	1.111	1.0798	
O9-H21	1.113	1.111	1.0767	
N10-H22	0.942	0.942	0.9511	
C11-C12	1.355	1.355	1.3801	
C12-H23	0.972	0.972	0.9485	
Bond angle(◦)				
C1-C2-C13	109.4997	110	111.999	
C2-C1-C14	109.4445	110	111.91	
C2-C1-C15	109.4607	110	108.621	
C13-C1-C14	109.4423	109	108.097	
C13-C1-C15	109.4624	109	107.963	
C14-C1-C15	109.5178	108.812	108.107	
C1-C2-C3	119.9998	115.1	117.707	123.3
C1-C2-C11	119.9995	121.4	122.124	
C3-C2-C11	120.0007	120	120.169	
C2-C3-C4	115.0005	115	120.052	117.3
C3-C4-C5	120.0004	123.5	123.005	123.3
C3-C4-C16	120.0055	118.249	116.158	
C5-C4-C16	119.9941	118.249	120.837	120.3
C4-C5-C6	119.9984	118.816	119.86	
C4-C5-O8	119.9977	122.366	118.272	120
C6-C5-O8	120.0039	118.816	121.867	120.2
C5-C6-C7	109.4954	109.5	108.302	
C5-C6-C17	109.4409	109.41	110.206	
C5-C6-C18	109.461	109.41	109.561	
C7-C6-C17	109.4425	106.7	110.016	
C7-C6-C18	109.4642	106.7	109.723	
C17-C6-C18	109.5234	114.965	109.022	
C6-C7-H19	119.9965	106.9	112.918	
C5-O8-O9	122.1903	120.432	121.777	
C5-O8-C11	115.6185	119.134	117.614	
O9-O8-C11	122.1912	120.432	120.606	
O8-O9-N10	109.5	109.5	107.784	
O8-O9-H20	109.4431	109.41	109.57	
O8-O9-H21	109.4604	109.41	109.878	
N10-O9-H20	109.4419	106.7	109.655	
N10-O9-H21	109.462	106.7	110.216	
O9-N10-H22	120.0015	114.965	112.786	
C2-C11-O8	129.3821	106.9	120.888	
C2-C11-C12	115.3088	119.999	121.437	
O8-C11-C12	115.309	119.999	117.673	

C11-C12-H23	120	108	115.152	
C13-C1-C2-C3	0	120	118.407	
C13-C1-C2-C11	180	-38.877	61.5377	
C14-C1-C2-C3	-119.9656	-0.0776	120.019	
C14-C1-C2-C11	60.0344	-158.95	60.063	
C15-C1-C2-C3	120.0002	-119.92	0.7439	
C15-C1-C2-C11	-59.9998	81.201	179.311	
C1-C2-C3-C4	180	-159.2	179.739	
C11-C2-C3-C4	0	0	0.3149	
C1-C2-C11-O8	180	157.862	179.93	
C1-C2-C11-C12	0	-21.565	0.5477	
C3-C2-C11-O8	0	0	0.1263	
C3-C2-C11-C12	180	-179.43	179.509	
C2-C3-C4-C5	0	0	0.3313	
C2-C3-C4-C16	180	-179.46	179.494	
C3-C4-C5-C6	180	-179.45	179.744	
C3-C4-C5-O8	0	0	0.1456	
C16-C4-C5-C6	0	0.0099	0.0729	
C16-C4-C5-O8	180	179.458	179.672	
C4-C5-C6-C7	180	0	109.606	
C4-C5-C6-C17	-60.0389	-116.61	130.004	
C4-C5-C6-C18	60.0001	116.615	10.0465	
O8-C5-C6-C7	0	-179.47	69.9778	
O8-C5-C6-C17	119.9611	63.9176	50.4126	
O8-C5-C6-C18	-119.9999	-62.853	170.37	
C4-C5-O8-O9	180	-179.42	179.341	
C4-C5-O8-C11	0	0	0.0453	
C6-C5-O8-O9	0	0.0281	1.069	
C6-C5-O8-C11	180	179.448	179.545	
C5-C6-C7-H19	180	60	176.156	
C17-C6-C7-H19	60.0399	178.315	55.6471	
C18-C6-C7-H19	-60.0021	-58.315	64.2925	
C5-O8-O9-N10	180	0	66.6979	
C5-O8-O9-H20	60.0356	-116.61	52.5714	
C5-O8-O9-H21	-60.003	116.615	173.179	
C11-O8-O9-N10	0	-179.41	112.67	
C11-O8-O9-H20	-119.9644	63.9732	128.061	
C11-O8-O9-H21	119.9997	-62.797	7.4526	
C5-O8-C11-C2	0	0	0.0534	
C5-O8-C11-C12	180	179.427	179.352	
O9-O8-C11-C2	180	179.42	179.34	
O9-O8-C11-C12	0	-1.1534	1.2544	
O8-O9-N10-H22	180	180	169.697	
H20-O9-N10-H22	-60.0348	-61.686	71.088	
H21-O9-N10-H22	60.0013	61.6854	49.7882	
C2-C11-N10-H23	0	-0.0001	5.2672	
O8-C11-C12-H23	180	-179.43	175.331	

Table 2: Observed and theoretical vibrational assignments of Pyridoxine at DFT-B3LYP methods

Experimental wavenumbers(cm^{-1})		Theoretical wavenumbers (cm^{-1})				Vibrational assignments
FTIR	FT Raman	B3LYP/6-311++G(d, p) scaled frequency	IR Intensity	B3LYP/6-311G(d, p) scaled frequency	IR Intensity	
		3340	82.3768	3343	76.292	νOH(93)
3322		3335	34.7256	3330	32.855	νOH(95)
3232	3233	3323	25.1097	3329	8.7531	νOH(88)
3086	3099	2767	4.4949	2735	25.576	νCH(96)
2815	2975	2726	3.0219	2728	3.7562	νCH(89)
	2934	2690	6.7272	2683	15.459	νCH(80)
	2901	2687	13.5951	2657	18.312	νCH(26)+β HCO (13)+t HCCC(34)

	2865	2648	19.6787	2647	23.291	νCH(81)
1827	2828	2622	44.4639	2637	28.936	νCH(68)
1731	1644	2610	29.3371	2610	31.687	νCH(87)
1625	1593	2590	57.5359	2609	57.536	νCH(43)+t HCCC(39)+ νOC(49)
1542	1449	1429	47.0951	1433	11.595	νNC(20)+ν CC(15)
1481	1419	1390	5.0108	1397	6.8949	βCCC(16)
1462	1392	1323	9.2249	1332	7.499	νNC(45)+ βHCH(14)
1415		1318	6.2901	1328	0.3592	νCH(26)+β HCH(14)
1387	1382	1296	5.9538	1323	7.2393	νCH(24)+βHOC(11)
1347	1358	1292	8.9902	1297	8.2987	βHCH(65)+t HCCC(12)
1275	1324	1288	5.5748	1291	15.98	βHCH(73)
	1294	1263	17.3594	1276	13.954	βHCH(53)
		1245	19.4872	1269	1.6948	βHCH(13)
	1232	1223	155.281	1246	146.06	νCC(11)+νOC(16)
1214	1217	1218	21.1512	1220	10.72	νOC(12)+βHCCC(12)
		1194	5.39	1164	18.08	βHOC(20)+βHCO(17)+tHCCC(31)
		1140	15.1402	1149	15.823	βHCN(15)+βHCH(11)
		1135	20.1946	1117	10.191	νCC(10)+νNC(23)+ βHOC(54)+βHCO(15)
		1112	22.9873	1114	52.727	νNC(29)+νCC(13)+βHCN(28)+ βHCH(14)
1088	1089	1097	4.9865	1108	38.829	βHOC(11)+tHCCC(11)
		1091	48.2515	1096	88.805	βHCH(19)
		1067	137.198	1081	66.63	νNC(15)+νOC(15)+νCC(10)
	1051	1051	35.5718	1074	54.38	βHOC(12)+βHCO(19)+βHCH(14)
989	988	1045	44.4614	1058	33.404	βHOC(49)+βHCO(25)
960	965	955	14.8706	964	32.191	βCCN(11)+tHOCC(27)
925	928	915	23.9894	917	1.7096	νCC(10)+νOC(31)
		910	2.0126	909	47.64	tHCCC(15)
		900	55.5185	895	30.223	νOC(21)+tHCCC(13)
870		885	77.7469	888	17.326	νOC(10)+tHCNC(11)
	865	850	20.0346	883	45.023	νOC(21)+tHCCC(12)+tOCCC(22)
		830	28.0112	831	10.165	βHCO(11)+tHOC(4)+tHOCC(62)+tHCCC(25)+γCCCC(12)
		804	5.6771	803	16.057	βHCN(13)+βHCH(11)+βCCN(13)+tHCCC(10)
793	751	774	18.6321	778	12.78	tHCNC(54)
748	724	685	27.5789	699	10.086	νHOC(28)+νCC(71)+tOCCC(11)+βCC(24)
684	691	652	13.4398	667	10.164	βCCN(13)+νCC(32)
591		618	6.4539	599	15.168	γOCCC(17)+γCCCC(10)
574		532	15.6078	559	1.8212	βCCC(10)+βCC(24)+tCCNC(13)+βCNC (14)
527	532	524	3.4792	537	2.1916	νCC(47)
474	476	492	6.8252	481	11.599	βCCN(13)+βCCC(16)+t CCNC(15)+γCCCC(10)
		453	13.0536	452	26.791	βCCN(11)+βOCC(10)+γ OCCC(16)
		437	9.1022	443	5.0358	tCCCN(11)+γ OCCC(14)
	402	334	5.6818	350	5.8827	νCCN(13) + νCCC(16) + tCCNC(15)+γ CCCC(10)
		319	3.2773	317	4.1677	βOCC(15)
	356	304	91.07	293	3.1406	t HOCC(55)
	328	283	11.5547	274	7.3981	βCCC(12)+βCCN(16)+βOCC(12)+β CNC (10)+βCC(79)
	287	263	4.0332	258	3.1396	βOCC(51)+βCCN(10)
	268	254	65.1849	246	40.036	βCCC(31)+βHOCC(12)+γ CCNC(17)
		223	58.7143	241	67.369	βOCC(23)+βCCN(19)+βCCC(10)+βHOCC(27)
		214	53.096	216	10.879	βHOC(14)+t HOCC(62)
		198	88.0318	203	178.02	βHOC(25)+t HOCC(31)
	169	161	13.8716	166	16.222	βCCN(10)+βCCC(13)+γ CCCC(11)
		114	0.5738	126	0.4287	βCCC(26)
	116	107	0.4218	114	5.2705	tHCCC(21)+tCCCN(13)
	85	87	2.7786	81	0.5874	βOCC(17)+t CNCC(50)+γ CCCC(11)
		66	0.8722	71	1.5404	tCCCN(11)+tCCNC(15)+γCCNC(16)
	63	52	2.5387	42	0.0731	νHOC(28)+tOCCC(11)

ν = stretching, β= bending, γ = out of plane bending, t = torsion

Table 3: Temperature dependent of thermodynamic properties Pyridoxine

S No	parameters	B3LYP/6-311++G(d, p),
1	E_{HOMO} (ev)	-0.24021
2	E_{LUMO} (ev)	-0.04197
3	$E_{HOMO-LUMO}$ energy gap (ev)	0.19824
4	Chemical hardness	0.14109
5	Softness (s)	3.543837
6	Electronegativity	0.09912
7	Electrophilicity(ω)	0.034814
8	Chemical potential	-0.09912

Table 4: Calculated energy values of Pyridoxine By B3LYP/6-311++G (d, p)

T (K)	S (J/mol.K)	Cp (J/mol.K)	ddH (kJ/mol)
100	306.52	93.56	5.92
200	389.85	150.91	18.27
298.15	459.5	201.26	35.55
300	460.75	202.2	35.93
400	525.78	251.55	58.65
500	586.68	294.68	86.02
600	643.67	330.36	117.34
700	696.86	359.57	151.88
800	746.51	383.75	189.08
900	792.91	404.03	228.5
1000	836.39	421.25	269.79

Table 5: The calculated Thermodynamic parameters of Pyridoxine

Parameters	B3LYP/6-311G(d, p)	RHF/6-31G(d, p)	B3LYP/6-311++G(d, p)
Zero-point vibrational energy (Kcal/Mol)	116.64819	125.83731	116.25942
Rotational constants (GHZ)	1.39516	0.06749	1.2672
	0.7452	0.03594	0.77179
	0.53496	0.02588	0.50218
Rotational temperatures (Kelvin)	0.06696	1.4062	0.06082
	0.03576	0.74888	0.03704
	0.02567	0.53919	0.0241
Molar capacity at constant volume (cal/Mol-kelvin)			
Total	45.856	42.957	46.114
Translational	2.981	2.981	2.981
Rotational	2.981	2.981	2.981
Vibrational	39.894	36.996	40.152
Electronic	0	0	0
Entropy(Cal/Mol-Kelvin)			
Total	109.551	107.581	109.797
Translational	41.283	41.283	41.283
Rotational	30.736	30.716	30.86
Vibrational	37.531	35.582	37.653
Electronic	0	0	0
Energy(kcal/Mol)			
Total	124.509	133.314	124.165
Translational	0.889	0.889	0.889
Rotational	0.889	0.889	0.889
Vibrational	122.732	131.536	122.387
Electronic	0	0	0

Table 6: Mulliken charge analysis by B3LYP/6-311++G (d, p), 6-311G(d, p) and RHF/6-31G(d, p)

S NO	Atoms	B3lyp/6-311++G(d, p)	RHF/6-31G	B3lyp/6-311G(d, p
1	C	-0.723204	-0.515199	-0.327924
2	C	-0.087482	0.247302	0.084731
3	N	-0.001575	-0.558834	-0.268364
4	C	-0.389312	0.039691	0.095452
5	C	-0.024804	-0.024804	-0.343514
6	C	-0.283335	-0.02701	0.095083
7	O	-0.749409	-0.749409	-0.451295
8	C	0.401036	0.074981	0.032227
9	C	-0.259017	-0.024066	0.146516
10	O	-0.25063	-0.756304	-0.415957
11	C	-0.141872	0.306256	0.188022
12	O	-0.236904	-0.805538	-0.383267
13	H	0.167046	0.167046	0.123744
14	H	0.196016	0.169968	0.115893
15	H	0.141771	0.220123	0.115881
16	H	0.137389	0.208278	0.071445
17	H	0.206727	0.21204	0.105169
18	H	0.185592	0.160169	0.10518
19	H	0.208667	0.40362	0.258233
20	H	0.190912	0.201838	0.10192
21	H	0.194819	0.213087	0.101936
22	H	0.278049	0.405513	0.217887
23	H	0.297113	0.43125	0.231002

Table 7: Experimental and calculated absorption wavelength (λ), excitation state, oscillator strength (f), electronic absorption value (ev) and transition of P yridoxine by TD-DFT method (B3LYP/6-311++G (d, p))

Excitation Singlet Acal.Wavelength (nm) Wavelength (nm) oscillator strength (f), Electronic absorption (ev) Transition

Excited State 1
45 -> 49 0.10642 204.34 6.0675 0.2853 HOMO↔ LUMO
45 -> 55 -0.24527 HOMO↔ LUMO+1
45 -> 58 -0.31263 HOMO↔ LUMO+2
45 -> 59 0.51592 HOMO↔ LUMO+3
Excited State 2
45 -> 46 0.49061 201.96 6.1390 0.0030 HOMO↔ LUMO
45 -> 47 0.20346 HOMO↔ LUMO+1
45 -> 48 0.22822 HOMO↔ LUMO+2
45 -> 53 0.25669 HOMO↔ LUMO+3
45 -> 56 -0.14950 HOMO↔ LUMO+4
45 -> 64 -0.15118 HOMO↔ LUMO+5
Excited State 3
44 -> 59 0.13237 184.71 6.7124 0.0204 HOMO↔ LUMO
45 -> 49 0.49264 HOMO↔ LUMO+1
45 -> 58 0.27106 HOMO↔ LUMO+2
45 -> 63 0.25495 HOMO↔ LUMO+3
45 -> 68 -0.12883 HOMO↔ LUMO+4
45 -> 69 -0.15732 HOMO↔ LUMO+5
45 -> 72 0.10433 HOMO↔ LUMO+6
45 -> 75 0.10068 HOMO↔ LUMO+7

Table 8: Second order perturbation theory analysis of FOCK matrix in NBO analysis for Pyridoxine

Donor(i)	TYPE	Acceptor(j)	Type	$E^{(2)a}$	$E(j)-E(i)^{b\ (a.u)}$	$F(I, j)^{c}$ (a.u)
Σ+	C1-C2	σ*	C2-N3	1.27	1.16	0.034
Σ	C1-C2	σ*	C2-C11	1.52	1.17	0.038
Σ	C1-C2	σ*	N3-C4	3.18	1.16	0.054
Σ	C1-C2	σ*	C8-C11	2.49	1.17	0.049
Σ	C1-H13	σ*	C2-N3	1.85	1.02	0.039
Σ	C1-H13	π*	C2-C11	3.28	0.52	0.04
Σ	C1-H14	σ*	C2-N3	0.88	1.01	0.027
Σ	C1-H14	σ*	C2-C11	3.85	1.03	0.056
Σ	C1-H14	π*	C2-C11	0.71	0.51	0.019
Σ	C1-H15	σ*	C2-N3	1.79	1.02	0.038

Σ	C1-H15	π*	C2-C11	2.3	0.52	0.034
Σ	C2-N3	σ*	C2-C11	1.54	1.33	0.041
Σ	C2-N3	σ*	C4-H16	2.45	1.22	0.049
Σ	C2-N3	σ*	C11-O12	2.64	1.15	0.049
Σ	C2-C11	σ*	C8-C9	3.12	1.12	0.053
Σ	C2-C11	σ*	C8-C11	3.58	1.24	0.06
Π	C2-C11	σ*	C1-H13	1.89	0.63	0.032
Π	C2-C11	σ*	C1-H15	2.63	0.63	0.04
Π	C2-C11	π*	N3-C4	17.48	0.27	0.062
Π	C2-C11	π*	C5-C8	14.09	0.38	0.066
Σ	N3-C4	σ*	C1-C2	3.68	1.21	0.06
Σ	N3-C4	σ*	C1-N3	0.93	1.31	0.031
Σ	N3-C4	σ*	C4-C5	1.32	1.34	0.038
Σ	N3-C4	σ*	C5-C6	1.87	1.24	0.043
Π	N3-C4	π*	C2-C11	21.04	0.3	0.074
Π	N3-C4	π*	C5-C8	12.35	0.4	0.064
Σ	C4-C5	σ*	N3-C4	0.8	1.2	0.028
Σ	C4-C5	σ*	C4-H16	0.62	1.1	0.023
Σ	C4-C5	σ*	C5-C6	2.06	1.12	0.043
Σ	C4-C5	σ*	C5-C8	10.81	1.63	0.118
Σ	C4-C5	σ*	C6-O7	0.73	1	0.024
Σ	C4-C5	σ*	C8-C9	7.39	1.09	0.08
Σ	C4-H16	σ*	C2-N3	3.84	1.02	0.056
Σ	C4-H16	σ*	C5-C8	3.26	1.46	0.062
Σ	C5-C6	σ*	N3-C4	2.68	1.14	0.05
Σ	C5-C6	σ*	C4-C5	1.89	1.16	0.042
Σ	C5-C6	σ*	C5-C8	8.08	1.57	0.101
Σ	C5-C6	σ*	C8-C9	0.66	1.03	0.023
Σ	C5-C6	σ*	C8-C11	7.28	1.15	0.082
σ	C5-C8	σ*	C4-C5	7.85	1.4	0.094
σ	C5-C8	σ*	C4-H16	1.1	1.28	0.034
σ	C5-C8	σ*	C5-C6	5.44	1.3	0.075
σ	C5-C8	σ*	C6-O7	0.69	1.18	0.026
σ	C5-C8	σ*	C8-C9	5.86	1.27	0.077
σ	C5-C8	σ*	C8-C11	8.06	1.39	0.094
σ	C5-C8	σ*	C11-O12	2.82	1.21	0.052
π	C5-C8	π*	C2-C11	15.55	0.32	0.065
π	C5-C8	π*	N3-C4	16.76	0.31	0.066
π	C5-C8	σ*	C6-H17	1.93	0.7	0.035
π	C5-C8	σ*	C6-H18	1.95	0.69	0.035
π	C5-C8	σ*	C9-H20	2.52	0.66	0.039
π	C5-C8	σ*	C9-H21	2.46	0.66	0.038
σ	C6-O7	σ*	C5-C8	1.52	1.76	0.047
σ	C6-H17	σ*	C4-C5	1.65	1.03	0.037
σ	C6-H17	π*	C5-C8	3.16	0.6	0.041
σ	C6-H17	σ*	O7-H19	2.5	0.96	0.044
σ	C6-H17	σ*	O10-H22	1.65	0.93	0.035
σ	C6-H18	σ*	C4-C5	1.69	1.03	0.037
σ	C6-H18	π*	C5-C8	3.16	0.6	0.041
σ	C6-H18	σ*	C6	1.8	0.93	0.037
σ	O7-H19	σ*	C6-H17	1.94	1.1	0.041
σ	C8-C9	σ*	C2-C11	1.97	1.17	0.043
σ	C8-C9	σ*	C4-C5	7.16	1.19	0.082
σ	C8-C9	σ*	C5-C6	0.58	1.08	0.023
σ	C8-C9	σ*	C5-C8	8.47	1.59	0.104
σ	C8-C9	σ*	C8-C11	1.56	1.17	0.038
σ	C8-C9	σ*	O10-H22	1.58	1.08	0.037
σ	C8-C11	σ*	C1-C2	2.59	1.1	0.048
σ	C8-C11	σ*	C2-C11	2.97	1.21	0.054
σ	C8-C11	σ*	C5-C6	6.6	1.13	0.077
σ	C8-C11	σ*	C5-C8	10.2	1.64	0.116
σ	C8-C11	σ*	C8-C9	1.56	1.1	0.037
σ	C8-C11	σ*	C9-O10	1.04	0.97	0.029
σ	C8-C11	σ*	C11-O12	0.5	1.04	0.02
σ	C8-C11	σ*	O12-H23	1.59	1.06	0.037
σ	C9-O10		C8	0.6	2.58	0.035
σ	C9-O10	σ*	C6-O7	1.38	1.16	0.036
σ	C9-O10	σ*	C8-C11	1.86	1.37	0.045
σ	C9-H20	σ*	C5-C8	1.4	1.48	0.041
σ	C9-H20	π*	C5-C8	3.38	0.64	0.044

σ	C9-H21	σ*	C5-C8	1.41	1.48	0.041
σ	C9-H21	π*	C5-C8	3.43	0.64	0.045
σ	O10-H22	σ*	C8-C9	2.22	1.16	0.046
σ	C11-O12	σ*	C2-N3	1.65	1.46	0.044
σ	C11-O12	σ*	C2-C11	0.82	1.47	0.031
σ	C11-O12	σ*	C5-C8	0.84	1.9	0.036
σ	C11-O12	σ*	C8-C11	0.62	1.47	0.027
σ	O12-H23	σ*	C8-C11	4.41	1.28	0.068
LP(1)	N3	σ*	C1-C2	1.45	0.77	0.03
LP(1)	N3	σ*	C2-C11	8.32	0.88	0.077
LP(1)	N3	σ*	C4-C5	7.88	0.9	0.076
LP(1)	N3	σ*	C4-C16	2.77	0.77	0.042
LP(1)	N3	σ*	C11-O12	0.71	0.7	0.02
LP(1)	O7	σ*	C5-C6	0.88	1.02	0.027
LP(1)	O7	σ*	C6-H17	2.44	0.97	0.044
LP(1)	O7	σ*	C6-H18	0.52	0.97	0.02
LP(2)	O7	σ*	N3-C4	0.75	0.8	0.022
LP(2)	O7	σ*	C5-C6	5.69	0.73	0.057
LP(2)	O7	σ*	C6-H18	5.42	0.67	0.054
LP(1)	O10	σ*	C6-H17	1.26	0.73	0.027
LP(1)	O10	σ*	C6-H18	1.04	0.72	0.024
LP(1)	O10	σ*	C9-H20	5.81	0.69	0.057
LP(1)	O10	σ*	C9-H21	5.14	0.69	0.053
LP(2)	O10	σ*	C6-O7	10.02	0.96	0.088
LP(2)	O10	σ*	C6-H18	0.5	1.03	0.02
LP(2)	O10	σ*	C8-C9	1.33	1.05	0.033
LP(2)	O10	σ*	C9-H21	0.58	0.99	0.022
LP(2)	O12	π*	C2-C11	28.67	0.35	0.095
π*	C2-C11	σ*	C1-C2	0.62	0.4	0.033
π*	C2-C11	σ*	C1-H13	1.24	0.35	0.044
π*	C2-C11	σ*	C1-H15	1.33	0.35	0.045
π*	C2-C11	π*	C5-C8	25.31	0.1	0.082
π*	N3-C5	π*	C5-C8	27.08	0.11	0.088
π*	C5-C8	σ*	C6-H17	1.8	0.28	0.053
π*	C5-C8	σ*	C6-H18	1.83	0.27	0.053
π*	C5-C8	σ*	C9-H20	1.53	0.24	0.045
π*	C5-C8	σ*	C9-H21	1.51	0.24	0.045